

Yu Guang (Orcid ID: 0000-0001-7918-0160)

mMrgprA3/mMrgprC11/hMrgprX1: potential therapeutic targets for allergic contact dermatitis induced pruritus in mice and human

Fengxian Li^{1,4} | Changming Wang^{2,3,4} | Danyou Hu^{2,3} | Xinyu Zhang^{2,3} | Ran Shen^{2,3} | Yuan Zhou^{2,3} | Yan Yang^{2,3} | Chan Zhu^{2,3} | Zongxiang Tang^{2,3} | Guang Yu^{2,3*}

¹Department of Anesthesiology, Zhujiang Hospital of Southern Medical University, Guangzhou, Guangdong, China

²School of Medicine & Holistic Integrative Medicine, Nanjing University of Chinese Medicine, Nanjing, Jiangsu, China

³Key Laboratory for Chinese Medicine of Prevention and Treatment in Neurological Diseases, Nanjing University of Chinese Medicine, Nanjing, Jiangsu, China

⁴These authors contribute equally to this work.

Correspondence

Guang Yu, School of Medicine & Holistic Integrative Medicine, Nanjing University of Chinese Medicine, Nanjing, Jiangsu, China.

Email: yuguang@njucm.edu.cn

CONFLICT OF INTEREST

The authors declare that they have no conflict of interest.

This article has been accepted for publication and undergone full peer review but has not been through the copyediting, typesetting, pagination and proofreading process which may lead to differences between this version and the [Version of Record](#). Please cite this article as doi: [10.1111/cod.14051](https://doi.org/10.1111/cod.14051)

This article is protected by copyright. All rights reserved.

Abstract

Background: Although the Mas-related G-protein-coupled receptors (Mrgprs) play essential roles in itch detection, their contribution to allergic contact dermatitis (ACD) associated itch remains unclear.

Objectives: To investigate whether Mrgprs are involved in ACD and whether Mrgprs can be identified as potential therapeutic targets.

Methods: *Mrgpr-cluster $\Delta^{-/-}$* mice and human *MrgprX1* (*hMrgprX1*) transgenic mice were applied to evaluate the function of Mrgprs in oxazolone-induced ACD.

Results: Utilizing ACD model, we find that *Mrgpr-cluster $\Delta^{-/-}$* mice display significantly reduced pruritus. Among 12 *Mrgprs* deleted in *Mrgpr-cluster $\Delta^{-/-}$* mice, the expression of *MrgprC11* and *MrgprA3* are significantly increased in ACD model, which also innervate the skin and spinal cord at higher-than-normal densities, the proportions of dorsal root ganglia neurons responding to bovine adrenal medulla peptide 8-22 and chloroquine are also remarkably increased in ACD model and result in enhancing itch behavior. To study the function of human Mrgprs in ACD-induced itch, we utilize *hMrgprX1* transgenic mice, which rescues the severe itch defect of *Mrgpr-cluster $\Delta^{-/-}$* mice in ACD model. Remarkably, pharmacological blockade of hMrgprX1 significantly attenuates ACD itch in *hMrgprX1* transgenic mouse.

Conclusions: Our study provides the first evidence that Mrgprs are involved in ACD induced chronic itch, which provides new avenues for itch management in ACD.

KEYWORDS

Allergic contact dermatitis, Mrgprs, sensory neurons, pruritus

Accepted Article

1. INTRODUCTION

Allergic contact dermatitis (ACD) is a common inflammatory skin disease associated with the persistent pruritus.¹ Previous epidemiological studies have suggested that the ACD patient population accounts for 20% of contact dermatoses.² Although itch is the major symptom of dermatitis, which often leads to excessive scratching, tissue damage and infection, and even insomnia, and despite decades of research, the mechanisms that drive strong pruritus in ACD are still largely unknown.^{3,4}

Itch sensation is initiated by the activation of sensory neurons whose cell bodies reside in the dorsal root ganglion (DRG) or trigeminal ganglion (TG).⁵ Several sensory neuron populations involved in itch detection are identified in recent studies, as well as GPCRs expressed by these neurons that acutely detect itchy stimuli. The best understood of these itch signaling cascade is histaminergic pathway, however, ACD associated chronic itch is commonly resistant to anti-histamines, underscoring the importance and clinical relevance of histamine-independent pruritic receptors.⁶

Mas-related G-protein-coupled receptors (Mrgprs) are the well-known itch receptors.⁷ As most of Mrgprs are expressed in primary sensory neurons (DRG and TG), the identification of the Mrgprs is an important advance in itch signal transmission.⁸ This family of receptors consists of > 20 functional members that are grouped into several subfamilies: MrgprA1-22, MrgprB1-13, MrgprC1-14, and MrgprD-G.^{7,9} MrgprA3 is identified as the receptor of the anti-malarial drug chloroquine (CQ) at the first and its activation can directly induce itch behavior.⁷ MrgprC11 mediates histamine-independent itch induced by bovine adrenal medulla peptide 8-22 (BAM) and SLIGRL-NH₂.¹⁰ MrgprA3 and MrgprC11 are largely co-expressed in DRG neurons, hence MrgprA3⁺ neurons also respond to MrgprC11

agonists. As histamine can also activate all CQ-sensitive neurons, MrgprA3⁺ neurons therefore respond to at least four different pruritogens.¹¹ Ablation of neurons expressing MrgprA3 attenuates dry skin and allergic itch, suggesting that MrgprA3⁺ neurons are necessary for the development of chronic itch. Therefore, MrgprA3⁺ sensory neurons are suggested as one of the major itch-sensing neuronal populations.¹²

Although it is well known that MrgprA3⁺ neurons are major players in the generation of itch, and Mrgprs are necessary in mouse models of SADBE-induced contact dermatitis and AEW-induced dry skin chronic itch,¹³ it is not clear which Mrgprs are involved in the generation of persistent oxazolone-induced chronic itch. Here we show that ACD related scratching is significantly reduced in *Mrgprs*-deficient (*Mrgpr-clusterΔ^{-/-}*) mice. Moreover, the percentage of MrgprC11⁺ and MrgprA3⁺ neurons as well as the density of MrgprA3⁺ fibers innervating skin and projecting to spinal cord are obviously increased in the context of ACD condition.

Refer to human relevance, human *MrgprX1* (*hMrgprX1*) receptor shares sequence homology with the mouse *MrgprA3* and *MrgprC11* subfamilies and *hMrgprX1* also expresses only in subsets of small-diameter sensory neurons in the DRG and TG. We use a transgenic mouse line in which the *hMrgprX1* gene is selectively expressed under the control of *MrgprC11* promoter in *Mrgpr-clusterΔ^{-/-}* mice.¹⁴ At the same time, ACD-associated itch behavior is rescued by introducing *hMrgprX1* into *Mrgpr-clusterΔ^{-/-}* mice.

Taken together, we provide evidence that mMrgprA3/mMrgprC11/hMrgprX1 play a critical role in mediating ACD associated itch, which provides potential therapeutic targets for anti-pruritus in clinical.

2. MATERIALS AND METHODS

2.1 Behavioral studies

The generation of *Mrgpr-clusterA^{-/-}*, *MrgprA3^{Cre-GFP}*, *Pirt^{GCaMP3/+}* and *hMrgprX1* transgenic mice are previously described.^{11,14-16} *ROSA26^{tdTomato}* mouse line (JAX#007909) is purchased from Jackson Laboratory. All the mice used have been backcrossed to C57BL/6 (wild-type, WT) mice for at least ten generations. 8- to 10-weeks old males (20-30 g) are used for all experiments. Animals are housed in and behavior experiments are performed in a controlled environment of 20°C-24°C, 45%-65% humidity, and with a 12-h day/night cycle. Animals are acclimated to the testing environment for 10 min before the initiation of behavior tests.

All behavioral tests and analyses are performed by experimenters blind to animal genotypes, and all experiments are performed under protocols approved by the Animal Care and Use Committee of Nanjing University of Chinese Medicine.

To induce chronic ACD, we shave and treat mice with oxazolone as previously described.¹⁷ Scratching behavior is recorded before the oxazolone treatment. Intradermal injection of chemicals are performed as previously described.¹⁸ Briefly, pruritic compounds are subcutaneously injected into the neck after acclimatization. Behavioral responses are videotaped for 45 min. For pharmacologically blocked hMrgprX1, JHU739 is injected with a concentration of 0.5 mM in 0.5% DMSO, and the scratching behavior is recorded immediately.

The bouts of scratching with the hind paw, directed toward the treated site, are counted. A bout of scratching is defined as a continuous scratching movement with a hind paw directed at the treated site until the hind paw is back on the floor or in the mouth.¹⁹

2.2 Culture of dissociated DRG neurons

DRG neurons from all spinal levels of mice are collected in cold DH10 (90% Dulbecco's modified Eagle's medium (DMEM)/F-12 (Sigma, D6421), 10% fetal bovine serum (FBS) (ThermoFisher, 10438026), penicillin (100 U/ml), and streptomycin (100 µg/ml) (ThermoFisher, 15140122)), and digested with enzyme solution (4U/ml dispase II, 342 U/ml collagenase Type I (ThermoFisher, 17100017) mixture in 1x Ca²⁺ free, Mg²⁺ free HBSS) at 37°C for 30 min with constant agitation. After trituration and centrifugation, cells are resuspended in DH10 and plated on glass coverslips coated with poly-D-lysine (0.5 mg/ml, Corning CB40210) and laminin (10 µg/ml, ThermoFisher, 23017015). Afterwards, seeded cells are allowed to attach onto coverslips at 37°C for 30 min, gently washed with warm DH10, and cultured in DH10 supplemented with 25ng/ml NGF (Corning, B40005A) and 50ng/ml GDNF (Sigma, SRP3200) in an incubator (95% O₂ and 5% CO₂) at 37°C. Cultured neurons are used within 24 hours after seeding.¹⁹

2.3 Calcium imaging

GFP signals from *Pirt^{GCaMP3/}* cultured neurons are imaged at 488nm excitation to detect intracellular Ca²⁺ transients. Test compounds are bath perfused into the imaging chamber through a gravity-based delivery system or directly applied into the bath by pipetting. Neurons are considered responsive if their fluorescence ratio is greater than or equal to 0.5 (fluorescence ratio= $\Delta F/F_0$, ΔF is the difference between maximum fluorescence and average baseline fluorescence, and F_0 is the average baseline fluorescence). Calcium imaging assays are performed with experimenters blind to the experimental grouping. All experiments are performed as at least triplicates.²⁰

2.4 Immunofluorescence staining

Immunostaining is performed as previously described.²¹ After the second and the fourth oxazolone treatment, mice are anesthetized with 1% sodium pentobarbital (50mg/kg, i.p.), and perfused with PBS (pH 7.4, 4°C) following by ice-cold 4% paraformaldehyde (pH 7.4).

DRG and spinal cord (C3-T10) are isolated from perfused mice, post-fixed in 4% paraformaldehyde (PFA) in PBS for 30 min and 2 h, respectively. Treated skin is post-fixed in 2% paraformaldehyde overnight. and cryoprotected in 30% sucrose at 4°C for 24 h. DRG and spinal cord are then embedded in optimum cutting temperature compound (OCT, Leica, Wetalar, Germany) and rapidly frozen at -20°C (CM 1950, Leica). Cryoembedded tissues are sectioned into 20 µm thick slices using sliding microtome (CM1950, Leica). Totally 1000 to 2000 sensory neurons from three mice are counted to quantify the percentage of tdTomato labeled MrgprA3⁺ neurons and MrgprC11 staining neurons.¹⁴ For skin and spinal cord section, 9 sections from three mice are analyzed to quantify the density of tdTomato labeled MrgprA3⁺ fibers by Image J software. To quantify the changes in the density of MrgprA3⁺ sensory fibers in skin, the length of MrgprA3⁺ sensory fibers per square millimeter is measured. To quantify the changes in the density of MrgprA3⁺ sensory fibers in spinal cord, we measure the mean gray value of MrgprA3⁺ sensory fibers by Image J software.

2.5 Real-Time Quantitative Reverse Transcription PCR

Total RNA of mouse DRG is extracted using RNeasy Mini Kit (Qiagen 74104). RNAs (0.5–1 µg) are reverse-transcribed using the High-Capacity cDNA Reverse Transcription Kits (ABI 4368814) according to the manufacturer's instructions. RT-PCR is carried out using SYBR Green (ABI 4385612) on a StepOnePlus thermocycler from ABI. Threshold cycles for each transcript are normalized to

GAPDH (ΔC_t). Calibrations and normalizations use the $2^{-\Delta\Delta C_t}$ method, where $\Delta\Delta C_t = [(C_t \text{ (target gene)} - C_t \text{ (reference gene)}) - [C_t \text{ (calibrator)} - C_t \text{ (reference gene)}]$. The primers for *Mrgprs* are listed in Table S1. All experiments are performed in triplicate.²⁰

2.6 Data Analysis

All data are presented as mean \pm standard error of mean (SEM). Statistical comparisons are made using ANOVA or unpaired Student's *t*-tests. All tests are carried out as 2-tailed tests. *P* values of less than 0.05 are considered statistically significant.

3. RESULTS

3.1 Involvement of *Mrgprs* in oxazolone-induced ACD itch

The oxazolone model is a well-established model for ACD, which induces dry scaly skin and atopic dermatitis-like skin inflammation characterized by acanthosis, parakeratosis (retention of nuclei in the stratum corneum), and immune cell infiltrate.²²

The schematic describing the generation of this model is shown in Figure 1A. Along with the development of skin barrier dysfunction and immune cell infiltration, this model generates itch-associated scratching behavior. After the second challenge, obvious scratching behavior is observed and there is a significant difference between the model and the control groups (39 ± 5.1 vs. 10 ± 2.5 , $P < 0.001$, $n=6$) (Figure 1B and D). After the fourth challenge, oxazolone treated mice develop severe chronic itch and scratching behavior is approximately 300 bouts/half hour (296 ± 19.0 vs. 10 ± 1.8) (Figure 1B and D). In this model, treated mice show severely disrupted skin barrier, which results in epidermal hyperplasia (Figure 1C and D). To determine whether *Mrgprs* are required for ACD itch, we examine the behavioral response of

Mrgpr-cluster $\Delta^{-/-}$ mice, in which twelve *Mrgprs* expressed by sensory neurons are deleted. We find that the deficiency of *Mrgprs* resulted in a significant reduction in itch behavior (Figure 1B). After the fourth challenge, compared with WT mice, *Mrgpr-cluster* $\Delta^{-/-}$ mice show strongly diminished itch behavior (162 ± 33.6 vs. 296 ± 19.0) (Figure 1B and F), suggesting that *Mrgprs* are required for itch in the ACD model. *Mrgpr-cluster* $\Delta^{-/-}$ mice, however, also develop epidermal hyperplasia and the thickness of their epidermal skin is not different from WT mice (Figure 1C and E).

3.2 ACD model increase *MrgprC11*⁺ and *MrgprA3*⁺ neurons in DRG

Mrgprs are involved in oxazolone induced ACD itchy, we then try to determine which *Mrgpr* is the primary mediator of this process. Among the 12 genes deleted in *Mrgpr-cluster* $\Delta^{-/-}$ mice, we find that *MrgprC11* and *MrgprA3* expressions are increased in ACD model, while other 10 *Mrgprs* neither show significant changes nor be detected by q-PCR (Table 1). Neurons that express *MrgprC11* also express *MrgprA3*, and *MrgprA3*⁺ neurons are thought to be itching specific.⁷ Since the expression of *MrgprC11* and *MrgprA3* is up-regulated in ACD, we examine if the percentages of *MrgprC11*⁺ and *MrgprA3*⁺ neurons are increased in ACD model. Compared with the control group, the percentage of *MrgprC11*⁺ neurons in DRGs is significantly increased in ACD model (4.3 ± 0.44 (control) vs. 8.3 ± 0.57 (after the second oxazolone challenge) vs. 7.3 ± 0.90 (after the fourth challenge) (Figure 2A and C). Using an *MrgprA3*-tdTomato reporter line, in which the BAC transgenic mouse line (*MrgprA3*^{GFP-Cre}) is crossed with a Cre-dependent *ROSA26*^{tdTomato} line, we find *MrgprA3* expression is also expanded in ACD. Compared with the control group, the percentage of *MrgprA3*⁺ neurons in DRGs is increased from 8.6 ± 1.11 (control) to 12.4 ± 0.90 (after the fourth challenge) in ACD model (Figure 2B and D).

Collectively, our data demonstrates that under ACD setting, the expression of MrgprC11 and MrgprA3 are significantly expanded.

Although the proportions of MrgprA3⁺ and MrgprC11⁺ neurons are increased in ACD model, the percentages of CGRP⁺ and NF200⁺ neurons are not changed in DRGs in this ACD model (Figure S1A-B).

3.3 ACD model increase MrgprA3⁺ fibers innervate to skin and spinal cord

MrgprC11 and MrgprA3 are co-expressed in DRG neurons, and constitute about 4-8% of sensory neurons.¹¹ Neurons that express these receptors also exclusively innervate the skin and spinal cord and are required for acute itch sensation induced by multiple pruritogens. No previous study, however, has investigated whether MrgprA3⁺ itch-sensing fibers are changed in the skin and spinal cord under ACD settings. Using the *MrgprA3-tdTomato* reporter mice, we visualize the peripheral and central fiber projections of MrgprA3⁺ neurons in skin and spinal cord, respectively. Consistent with our previous observation that the proportion of MrgprC11⁺ and MrgprA3⁺ neurons is increased after oxazolone treatment, the density of MrgprA3⁺ fibers in the skin is nearly doubled (Figure 3A-B). Peptidergic and nonpeptidergic fibers innervate laminae I and II outer layer (Ilo) and lamina II inner layer (Ili) on the spinal cord, respectively. Likewise, we find that MrgprA3⁺ fiber density is increased in the spinal cord in the ACD model, and that these fibers are co-localized with both peptidergic CGRP⁺ fibers and nonpeptidergic IB4⁺ fibers (Figure 3C-E).

3.4 ACD model increase neuronal sensitivity to BAM and CQ

In addition to molecular characterization, we monitor the response of cultured DRG neurons to BAM and CQ *ex vivo* using *Pirt^{GCaMP3/+}* mouse, in which genetically encoded calcium indicator, GCaMP3, is expressed by most sensory neurons. Indeed, our studies show that the proportion of DRG neurons that respond to BAM is

Accepted Article

significantly increased in *Pirt^{GCaMP3/+}* mice treated with oxazolone, compare with control mice (4.5 ± 0.32 (control) vs. 6.4 ± 0.60 (after second challenge) vs. 7.6 ± 0.47 (after fourth challenge)) (Figure 4A-B). Likewise, the proportion of DRG neurons that responded to CQ is also increased in ACD (Figure 4C).

3.5 BAM and CQ induce more scratching response in ACD model mice

Hyperkinesia is a common symptom of chronic itch patients. To test whether the enhanced neuronal sensitivity to BAM and CQ leads to increased itch in ACD, low doses of BAM (20 μ g in 50 μ L) and CQ (50 μ g in 50 μ L) are used to induce scratching behavior (Figure 5A). The scratching behavior in response to low doses of BAM and CQ after two times oxazolone challenge (before the onset of oxazolone-induced spontaneous itch) is measured. Compared to high concentration BAM (50 μ L of 1 mM) and CQ (200 μ g in 50 μ L, 8 mM),^{7,23} low doses of BAM and CQ induce fewer scratching behavior in control mice (Figure 5B and D, left), however, in ACD mice, BAM and CQ induce robust scratching behavior (Figure 5B and D, right). Importantly, the changed scratching number (difference between the scratching number post-drug injection and pre-drug injection) is significantly increased in ACD mice. Both BAM (55 ± 7.9 vs. 27 ± 3.8 , Figure 5C) and CQ (111 ± 15.4 vs. 59 ± 8.9 , Figure 5E) induce more scratching behavior in ACD mice.

3.6 *hMrgprX1* rescues diminished itch response of *Mrgpr-clusterA^{-/-}* mice in ACD

In humans, *MrgprX1* shares sequence homology with the mouse *MrgprA3* and *MrgprC11* and is also only expressed in subsets of small-diameter sensory neurons in DRG and TG, *hMrgprX1* is considered as a new target for itch management.²⁴ Further studies are required to investigate the involvement of *hMrgprX1* in chronic itch conditions. *hMrgprX1* transgenic mice rescue calcium response to BAM of DRG neurons (Figure 6B), the scratching behavior induced by BAM injection also

Accepted Article

significantly increased in *hMrgprX1* transgenic mice (Figure 6C). Importantly, the transgenic expression of *hMrgprX1* rescues the itch defects of *Mrgpr-clusterΔ^{-/-}* mice in ACD, and the scratch behavior between the WT and the *hMrgprX1* mice were similar (267 ± 19 vs. 251 ± 17) in this ACD model (Figure 6A and D). Our results suggest that hMrgprX1 serves as a primary itch receptor mediating human ACD.

To determine whether hMrgprX1 is a potential drug target for ACD itch management, we pharmacologically block the function of hMrgprX1 by using an antagonist (JHU739)²⁵ and the IC₅₀ of JHU739 to hMrgprX1 is checked by calcium imaging test (Figure S2). According to our result, JHU739 can significantly attenuate ACD-associated itch (Figure 6A and E), which emphasizes the importance of hMrgprX1 in ACD itch and JHU739 could be a potential therapeutic drug for ACD.

4. DISCUSSION

The prevalent resistance of pruritic diseases to anti-histamines, as exemplified by ACD, argues strongly for the involvement of histamine-independent pruritic receptors in chronic itch and for the development of therapies that target histamine-independent itch pathways for the management of these conditions.⁶ Recent studies have identified several members of the Mrgpr family as new itch receptors. CQ, an anti-malaria drug, activates MrgprA3 to induce itch.⁷ MrgprC11 is involved in BAM8-22, SLIGRL, and cathepsin S-induced itch.^{7,10,26} MrgprD mediates β-alanine-induced itch.²⁷ Likewise in humans, two MRGPR members X1 and X4 have been demonstrated to mediate itch sensation evoked by CQ and cholestasis respectively.^{7,28,29}

To study the function of Mrgprs in ACD, used the *Mrgpr-clusterΔ^{-/-}* mice, in which 12 Mrgprs are knock out, oxazolone-induced scratching behavior is significantly reduced in these mice. *Mrgpr-clusterΔ^{-/-}* mice do not show differences in epidermal

hyperplasia in this ACD model, this is likely due to the fact that Mrgprs are expressed only in DRG and TG, and the main function of Mrgprs is to detect and transmit itch and pain sensations. Although the scratching behavior of *Mrgpr-clusterΔ^{-/-}* mice in ACD model is significantly decreased in our study, there are still have 150 bouts in 30 min. We assume that this intensity of scratching still can cause hyperplasia. To determine the key Mrgprs for chronic itch in the ACD model, the expression of all 12 *Mrgprs* are analyzed by q-PCR. We find that the expression of *MrgprA3* and *MrgprC11* are significantly increased. Previous studies have identified *MrgprC11* and *MrgprA3* as itch receptors, and the expressions of these receptors are largely overlapped in DRG neurons.⁷ To further clarify the change in *MrgprA3* and *MrgprC11* expression in ACD settings, the percentages of MrgprA3⁺ and MrgprC11⁺ neurons are calculated. Consistent with molecular results, the proportions of MrgprA3⁺ and MrgprC11⁺ neurons are significantly increased in the ACD mice. Besides the increased proportion of itch neurons, enhanced density of sensory fibers at peripheral and central innervated zones is also essential for the development of chronic itch. Skin biopsies from atopic dermatitis patients show enhanced intraepidermal fiber density, as labeled by PGP9.5.³⁰ The elevated proportion of MrgprA3⁺ neurons results in a significant increase in the density of MrgprA3⁺ fibers in the skin and spinal cord. Chronic itch is often accompanied by sensitization of itch-detecting receptors. Consistent with this, we find that the itch responses induced by CQ and BAM are more pronounced in ACD mice. Our results suggest that both MrgprA3 and MrgprC11 are involved in the development of ACD itch.

In humans, *MrgprX1* shares sequence homology with the mouse *MrgprA3* and *MrgprC11*, and *hMrgprX1* is expressed only in subsets of small-diameter sensory

neurons in DRG and trigeminal ganglia.⁷ To demonstrate that our observations of *MrgprA3* and *MrgprC11* changes in mice reflect human ACD, we generate *hMrgprX1* mice, in which *hMrgprX1* is introduced into the *Mrgpr-clusterΔ^{-/-}* mice. The transgenic expression of this *hMrgprX1* rescues the itch defects of *Mrgpr-clusterΔ^{-/-}* mice in ACD model. Our results further show that *hMrgprX1* may be an important target for chronic itch treatment in human, as pharmacological blockade of hMrgprX1 by an antagonist (JHU739) significantly attenuate ACD-associated itch. Although JHU739 can inhibit the function of hMrgprX1, we still have no enough evidence to prove that JHU739 is a specific antagonist of MrgprX1. We need more data to evaluate its potential side effects in the condition of systemic administration. We can detect the side effects and toxicity of JHU739 in mice in the condition of systemic administration in subsequent research. We believe that topical administration has better safety, and also more conducive to assessing its inhibitory effects of itching caused by ACD, so JHU739 is injected into model mice in this manuscript, and the scratching behavior is recorded immediately. There are still many parameters that need to be detected, before JHU739 can be developed into an effective anti-pruritus drug.

Together, our findings demonstrate the indispensable role of mouse *MrgprA3* and *MrgprC11*, and human hMrgprX1 receptors in ACD-associated itch. These data provide the neural mechanism for oxazolone-induced ACD itch and pave an avenue for the development of novel and effective itch management and therapy in the future.

ACKNOWLEDGEMENTS

This work was supported by the Natural Science Foundation of Jiangsu Province (Grant no. BK20151571 to GY), the Jiangsu Provincial Key Research and

Development Program (Grant no. BE2017728 to GY). Thanks for Dr Xinzhong Dong for providing the hMrgprX1 transgenic mice. The antibody of MrgprC11 and the JHU739 (antagonist of hMrgprX1) are also provided by Dr Xinzhong Dong.

AUTHOR CONTRIBUTIONS

Fengxian Li: Conceptualization; investigation; writing-original draft. **Changming Wang:** Conceptualization; investigation. **Danyou Hu:** Investigation. **Xinyu Zhang:** Formal analysis; investigation. **Ran Shen:** Investigation. **Yuan Zhou:** Investigation. **Yan Yang:** Investigation. **Chan Zhu:** Investigation. **Zongxiang Tang:** Methodology; supervision. **Guang Yu:** Conceptualization; funding acquisition; supervision; writing-original draft; writing-review and editing; resources; supervision; validation.

DATA AVAILABILITY STATEMENT

The data that support the findings of this study are available from the corresponding author upon reasonable request

References

1. Bilimoria SN, Lio PA. Biologics for Allergic Dermatologic Diseases. *Current allergy and asthma reports*. Jun 6 2020;20(8):35. <https://doi.org/10.1007/s11882-020-00923-7>.
2. Murphy PB, Hooten JN, Atwater AR, Gossman W. Allergic Contact Dermatitis. *StatPearls*. Treasure Island (FL): StatPearls Publishing Copyright © 2020, StatPearls Publishing LLC.; 2020.
3. Hu XQ, Tang Y, Ju Y, et al. Scratching damages tight junctions through the Akt-claudin 1 axis in atopic dermatitis. *Clinical and experimental dermatology*. Jul 15 2020;46(1):74-81. <https://doi.org/10.1111/ced.14380>.
4. Wang X, Shi XD, Li LF, Zhou P, Shen YW. Classification and possible bacterial infection in outpatients with eczema and dermatitis in China: A cross-sectional and

- multicenter study. *Medicine*. Sep 2017;96(35):e7955.
<https://doi.org/10.1097/MD.0000000000007955>.
5. Xing Y, Chen J, Hilley H, Steele H, Yang J, Han L. Molecular Signature of Pruriceptive MrgprA3(+) Neurons. *The Journal of investigative dermatology*. Oct 2020;140(10):2041-2050. <https://doi.org/10.1016/j.jid.2020.03.935>.
 6. Davidson S, Giesler GJ. The multiple pathways for itch and their interactions with pain. *Trends Neurosci*. Dec 2010;33(12):550-558. <https://doi.org/10.1016/j.tins.2010.09.002>.
 7. Liu Q, Tang Z, Surdenikova L, et al. Sensory neuron-specific GPCR Mrgprs are itch receptors mediating chloroquine-induced pruritus. *Cell*. Dec 24 2009;139(7):1353-65. <https://doi.org/10.1016/j.cell.2009.11.034>.
 8. Arifuzzaman M, Mobley YR, Choi HW, et al. MRGPR-mediated activation of local mast cells clears cutaneous bacterial infection and protects against reinfection. *Science advances*. Jan 2019;5(1):eaav0216. <https://doi.org/10.1126/sciadv.aav0216>.
 9. Liu Q, Vrontou S, Rice FL, Zylka MJ, Dong X, Anderson DJ. Molecular genetic visualization of a rare subset of unmyelinated sensory neurons that may detect gentle touch. *Nature neuroscience*. Aug 2007;10(8):946-8. <https://doi.org/10.1038/nn1937>.
 10. Liu Q, Weng HJ, Patel KN, et al. The distinct roles of two GPCRs, MrgprC11 and PAR2, in itch and hyperalgesia. *Science signaling*. Jul 12 2011;4(181):ra45. <https://doi.org/10.1126/scisignal.2001925>.
 11. Han L, Ma C, Liu Q, et al. A subpopulation of nociceptors specifically linked to itch. *Nature neuroscience*. Feb 2013;16(2):174-82. <https://doi.org/10.1038/nn.3289>.
 12. Xing Y, Chen J, Hilley H, Steele H, Yang J, Han L. Molecular Signature of Pruriceptive MrgprA3(+) Neurons. *The Journal of investigative dermatology*. Mar 29 2020. <https://doi.org/10.1016/j.jid.2020.03.935>.
 13. Zhu Y, Hanson CE, Liu Q, Han L. Mrgprs activation is required for chronic itch conditions in mice. *Itch (Phila)*. Dec 2017;2(3). <https://doi.org/10.1097/itx.0000000000000009>.

14. Li Z, Tseng PY, Tiwari V, et al. Targeting human Mas-related G protein-coupled receptor X1 to inhibit persistent pain. *Proc Natl Acad Sci U S A*. Mar 7 2017;114(10):E1996-E2005. <https://doi.org/10.1073/pnas.1615255114>.
15. Liu Q, Tang Z, Surdenikova L, et al. Sensory Neuron-Specific GPCR Mrgprs Are Itch Receptors Mediating Chloroquine-Induced Pruritus. *Cell*. Dec 9 2009:1353-1365.
16. Kim YS, Chu Y, Han L, et al. Central terminal sensitization of TRPV1 by descending serotonergic facilitation modulates chronic pain. *Neuron*. Feb 19 2014;81(4):873-887. <https://doi.org/10.1016/j.neuron.2013.12.011>.
17. Liu B, Escalera J, Balakrishna S, et al. TRPA1 controls inflammation and pruritogen responses in allergic contact dermatitis. *FASEB journal : official publication of the Federation of American Societies for Experimental Biology*. Sep 2013;27(9):3549-63. <https://doi.org/10.1096/fj.13-229948>.
18. Shimada SG, LaMotte RH. Behavioral differentiation between itch and pain in mouse. *Pain*. Oct 31 2008;139(3):681-7. <https://doi.org/10.1016/j.pain.2008.08.002>.
19. Yu G, Yang N, Li F, et al. Enhanced itch elicited by capsaicin in a chronic itch model. *Molecular pain*. 2016;12. <https://doi.org/10.1177/1744806916645349>.
20. Hu D, Wang C, Li F, et al. A Combined Water Extract of Frankincense and Myrrh Alleviates Neuropathic Pain in Mice via Modulation of TRPV1. *Neural plasticity*. 2017;2017:3710821. <https://doi.org/10.1155/2017/3710821>.
21. Huang CC, Kim YS, Olson WP, et al. A histamine-independent itch pathway is required for allergic ocular itch. *J Allergy Clin Immunol*. Apr 2016;137(4):1267-70 e1-6. <https://doi.org/10.1016/j.jaci.2015.08.047>.
22. Liu B, Tai Y, Liu B, Caceres AI, Yin C, Jordt SE. Transcriptome profiling reveals Th2 bias and identifies endogenous itch mediators in poison ivy contact dermatitis. *JCI insight*. Jun 11 2019;5(14). <https://doi.org/10.1172/jci.insight.124497>.
23. Shi H, Yu G, Geng X, et al. MrgprA3 shows sensitization to chloroquine in an acetone-ether-water mice model. *Neuroreport*. Dec 6 2017;28(17):1127-1133. <https://doi.org/10.1097/WNR.0000000000000877>.

24. Prchalova E, Hin N, Thomas AG, et al. Discovery of Benzamidine- and 1-Aminoisoquinoline-Based Human MAS-Related G-Protein-Coupled Receptor X1 (MRGPRX1) Agonists. *Journal of medicinal chemistry*. Sep 26 2019;62(18):8631-8641. <https://doi.org/10.1021/acs.jmedchem.9b01003>.
25. Kunapuli P, Lee S, Zheng W, et al. Identification of small molecule antagonists of the human mas-related gene-X1 receptor. *Analytical biochemistry*. Apr 1 2006;351(1):50-61. <https://doi.org/10.1016/j.ab.2006.01.014>.
26. Reddy VB, Sun S, Azimi E, Elmariah SB, Dong X, Lerner EA. Redefining the concept of protease-activated receptors: cathepsin S evokes itch via activation of Mrgprs. *Nature communications*. Jul 28 2015;6:7864. <https://doi.org/10.1038/ncomms8864>.
27. Liu Q, Sikand P, Ma C, et al. Mechanisms of itch evoked by beta-alanine. *J Neurosci*. Oct 17 2012;32(42):14532-7. <https://doi.org/10.1523/JNEUROSCI.3509-12.2012>.
28. Meixiong J, Vasavda C, Snyder SH, Dong X. MRGPRX4 is a G protein-coupled receptor activated by bile acids that may contribute to cholestatic pruritus. *Proc Natl Acad Sci U S A*. May 21 2019;116(21):10525-10530. <https://doi.org/10.1073/pnas.1903316116>.
29. Yu H, Zhao T, Liu S, et al. MRGPRX4 is a bile acid receptor for human cholestatic itch. *eLife*. Sep 10 2019;8. <https://doi.org/10.7554/eLife.48431>.
30. Kubanov AA, Katunina OR, Chikin VV. Expression of Neuropeptides, Neurotrophins, and Neurotransmitters in the Skin of Patients with Atopic Dermatitis and Psoriasis. *Bulletin of experimental biology and medicine*. Jul 2015;159(3):318-22. <https://doi.org/10.1007/s10517-015-2951-4>.

Table 1 Fold increase in expression of *Mrgprs* in ACD model.

Gene	<i>A1</i>	<i>A2</i>	<i>A3</i>	<i>A4</i>	<i>A10</i>	<i>A12</i>	<i>A14</i>	<i>A16</i>	<i>A19</i>	<i>B4</i>	<i>B5</i>	<i>C11</i>
2th	ns	ns	1.9±0.20*	-	-	-	-	-	-	ns	ns	2.8±0.32*
4th	ns	ns	1.1±0.06	-	-	-	-	-	-	ns	ns	2.3±0.20*

ns, no significance; -, no signal; *, $P < 0.05$.

Figure Legends

FIGURE 1 Decreased itch behavior in *Mrgpr-cluster* $\Delta^{-/-}$ mice. (A) Schematic of the oxazolone-induced ACD model. (B) WT mice develop significant scratching behavior in the ACD model (n=6 per group). (C) HE staining of skin sections of WT and *Mrgpr-cluster* $\Delta^{-/-}$ mice (n = 3 per group). (D) ACD model results in scaly epidermal hyperplasia, indicated by HE staining (n = 3 per group). (E) There are no significantly difference in epidermis thickness between WT and *Mrgpr-cluster* $\Delta^{-/-}$ mice after 2 times oxazolone treatment (n = 3 per group). (B, F) WT mice display significantly stronger scratching behavior than *Mrgpr-cluster* $\Delta^{-/-}$ mice in oxazolone-induced ACD model (n=6 for each genotype). The scale bar represents 50 μ m. **, $P < 0.01$; ***, $P < 0.001$.

FIGURE 2 ACD Increases proportion of *MrgprC11* $^{+}$ and *MrgprA3* $^{+}$ neurons in DRG. (A, C) Immunostaining shows a significant up-regulation of *MrgprC11* $^{+}$ neurons in the DRGs of oxazolone-treated mice (n = 3 per group). (B, D) The proportion of *MrgprA3* $^{+}$ neurons in DRG of oxazolone-treated mice is increased (n = 5 per group). The scale bar represents 100 μ m. *, $P < 0.05$; **, $P < 0.01$.

FIGURE 3 The density of *MrgprA3* $^{+}$ fibers innervate in the skin and spinal cord is increased in the ACD. (A) The white dashed line outlines the epidermis and where *MrgprA3* $^{+}$ itch-sensing fibers innervate. The white arrow points to the *MrgprA3* $^{+}$ fibers. (B) The density of *MrgprA3* $^{+}$ fibers innervate in the skin is nearly doubled after oxazolone treatment (n = 3 per group). (C, D) *MrgprA3* $^{+}$ itch-sensing fibers innervate in spinal cord. (E) The density of *MrgprA3* $^{+}$ fiber innervation in the spinal cord is also increased after oxazolone treatment (n = 3 per group). The scale bar represents 50 μ m. *, $P < 0.05$; ***, $P < 0.001$.

FIGURE 4 ACD enhances neuronal activity to BAM and CQ. (A) Representative images of GCaMP3 fluorescence in cultured DRG neurons from control and ACD mice, at baseline and after treatment with 5 μ M BAM and 1 mM KCl. (B) The proportion of DRG neurons sensitive to BAM is significantly increased in ACD mice (n = 6 per group). (C) The proportion of DRG neurons sensitive to CQ is also increased in ACD mice (n = 6 per group). The scale bar represents 50 μ m. *, $P < 0.05$; **, $P < 0.01$; ***, $P < 0.001$.

FIGURE 5 Sensitization of the scratching response to BAM and CQ in ACD model.

(A) The protocol of BAM or CQ induced scratching behavior in ACD model. (B) Quantification of scratching behavior following BAM (20 μ g/50 μ l) intradermal injection in control (left) and ACD model (right) mice (n = 8 per group). (C) BAM induces stronger scratching behavior in ACD model mice compared to control mice. (D) Quantification of scratching behavior following CQ (50 μ g/50 μ l) intradermal injection in control (left) and ACD model (right) mice (n = 6 per group). (E) CQ also induces stronger scratching behavior in ACD model mice (n = 6 per group). *, $P < 0.05$; **, $P < 0.01$; ***, $P < 0.001$.

FIGURE 6 *hMrgprX1* rescues the diminished itch behavior in *Mrgpr-cluster* $\Delta^{-/-}$ mice in ACD model. (A) Schematic of the ACD model and JHU739 treatment. (B) The transgenic expression of *hMrgprX1* rescues the calcium response defects in DRG neurons of *Mrgpr-cluster* $\Delta^{-/-}$ mice. (C) The transgenic expression of *hMrgprX1* rescues BAM-induced scratching behavior defects of *Mrgpr-cluster* $\Delta^{-/-}$ mice. (D) The transgenic expression of *hMrgprX1* rescues the itch defects of *Mrgpr-cluster* $\Delta^{-/-}$ mice in AD model (***, compared with WT mice; ###, compared with *Mrgpr-cluster* $\Delta^{-/-}$ mice). (E) Pharmacological blockade *hMrgprX1* function by intradermal injection of JHU739 (500 μ M/50 μ l) significantly attenuates ACD-induced itch (n = 8 per group).

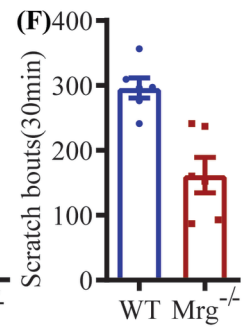
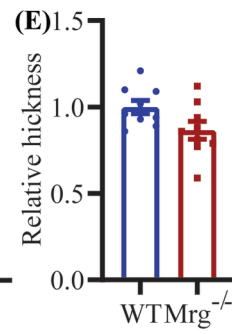
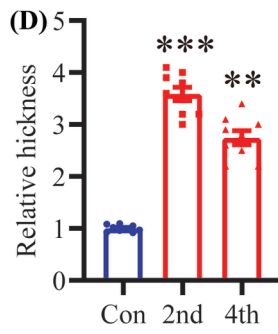
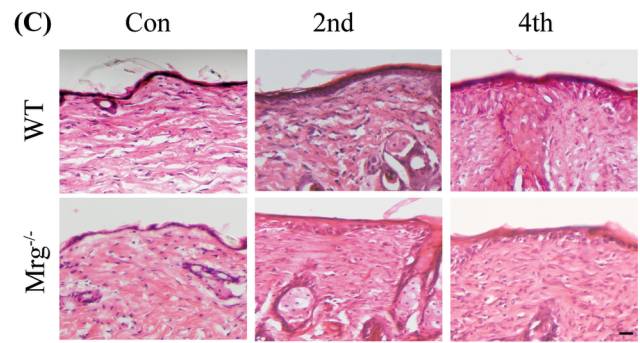
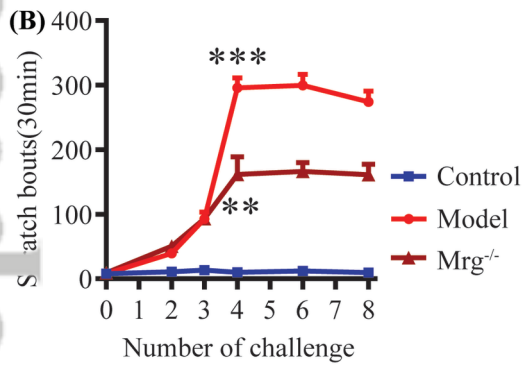
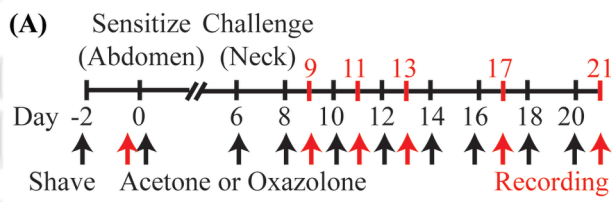
******, $P < 0.01$; *******, $P < 0.001$; **###**, $P < 0.001$.

Accepted Article

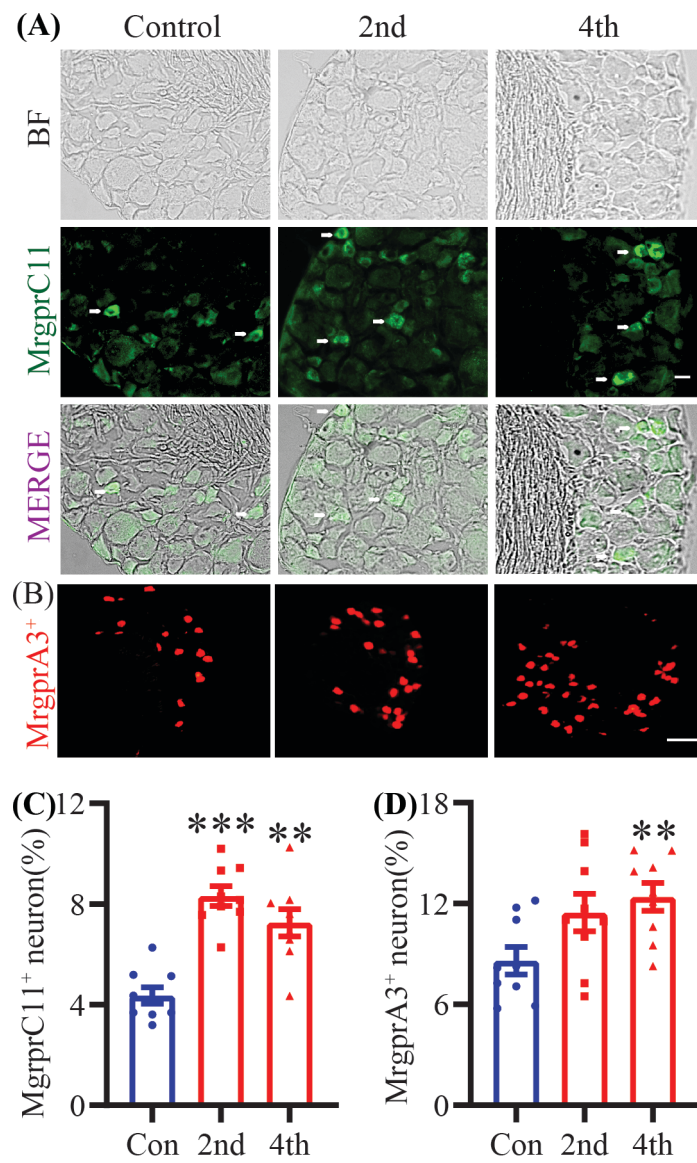
Supplementary figure legends

FIGURE 1 CGRP and NF200 staining of ACD model. (A) The percentage of CGRP⁺ neurons in ACD model was not changed. (B) The percentage of NF200⁺ neurons in ACD model was not changed. The scale bar represents 50 μ m.

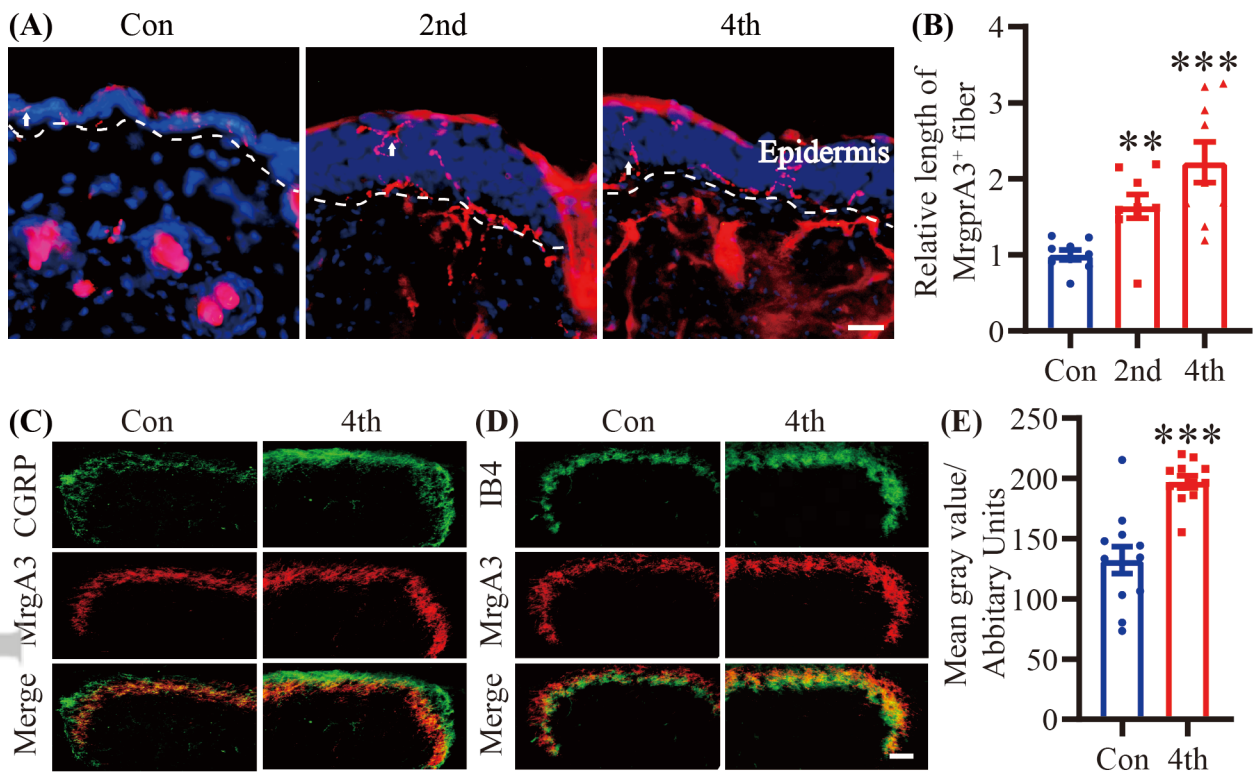
FIGURE 2 The IC₅₀ of JHU739 to hMrgrX1 was checked by calcium imaging test.



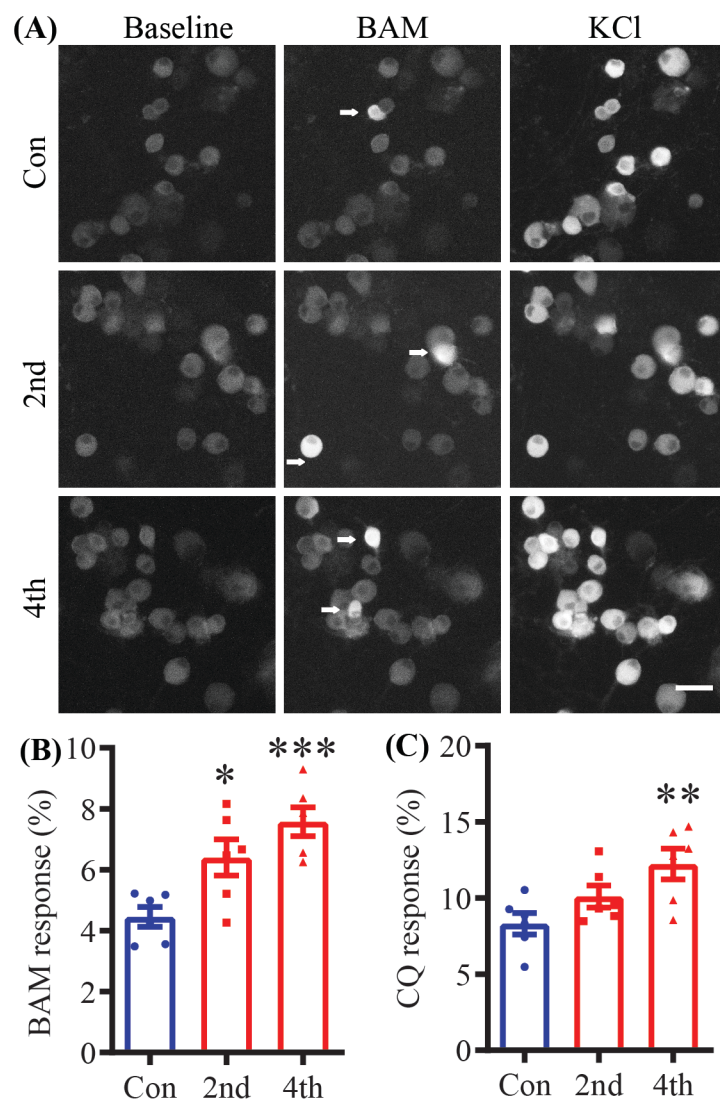
COD_14051_Figure 1.tif



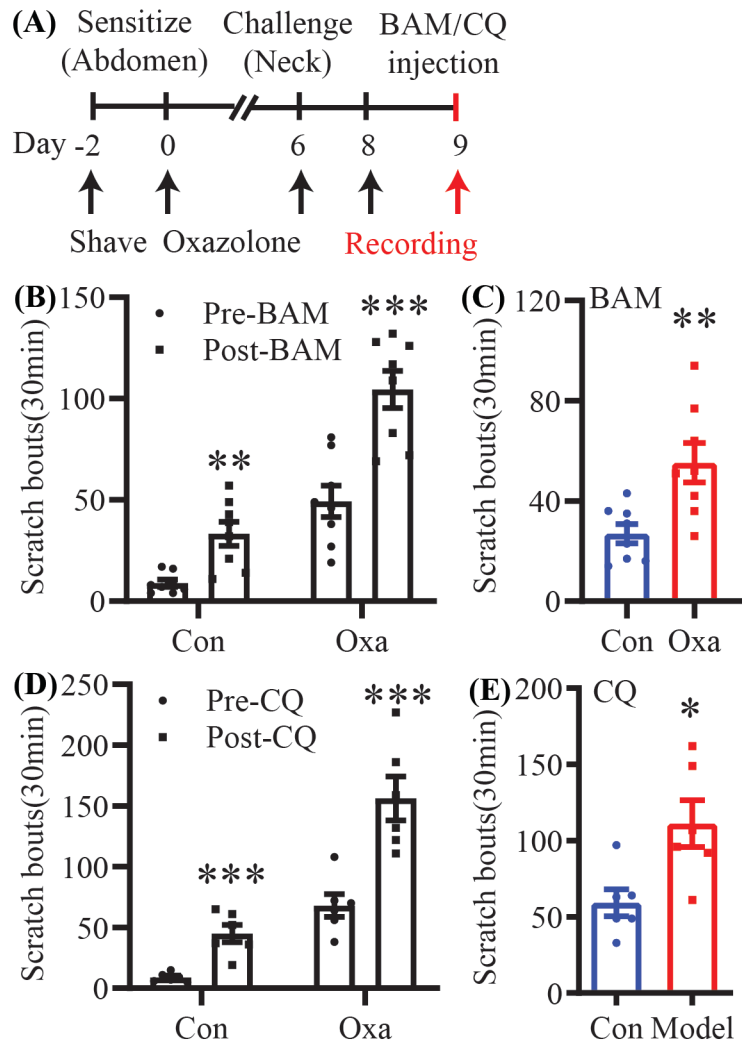
COD_14051_Figure2-4 mrgprc11 and mrgpra3+ neuron staining.tif



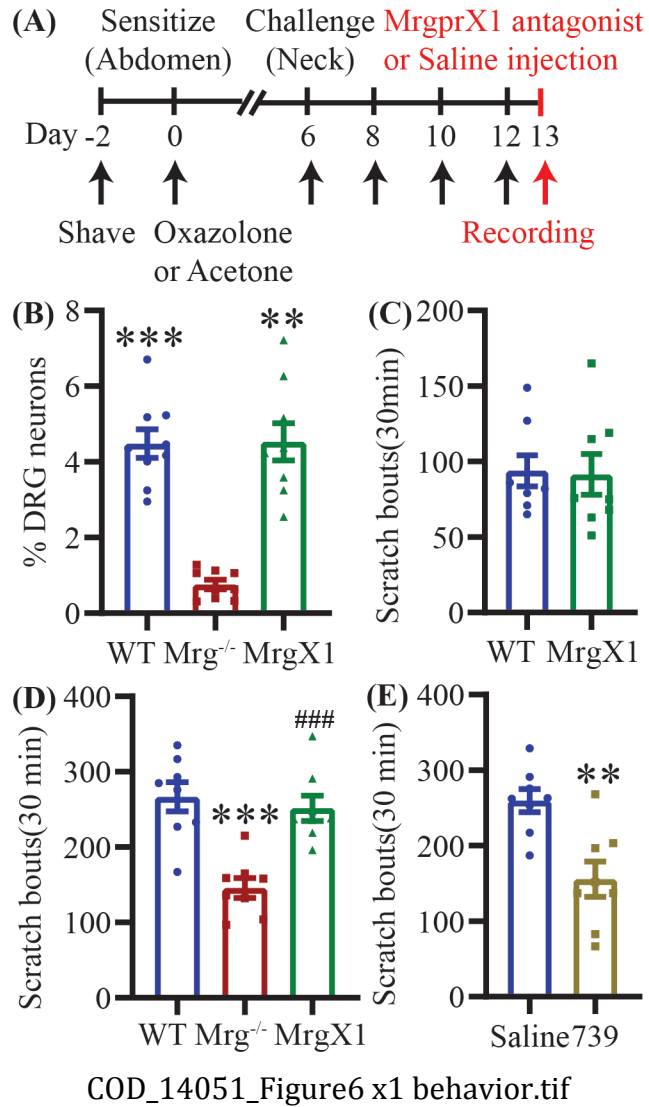
COD_14051_Figure3 mrgpra3+ NEURON spinal cord and skin-10.tif

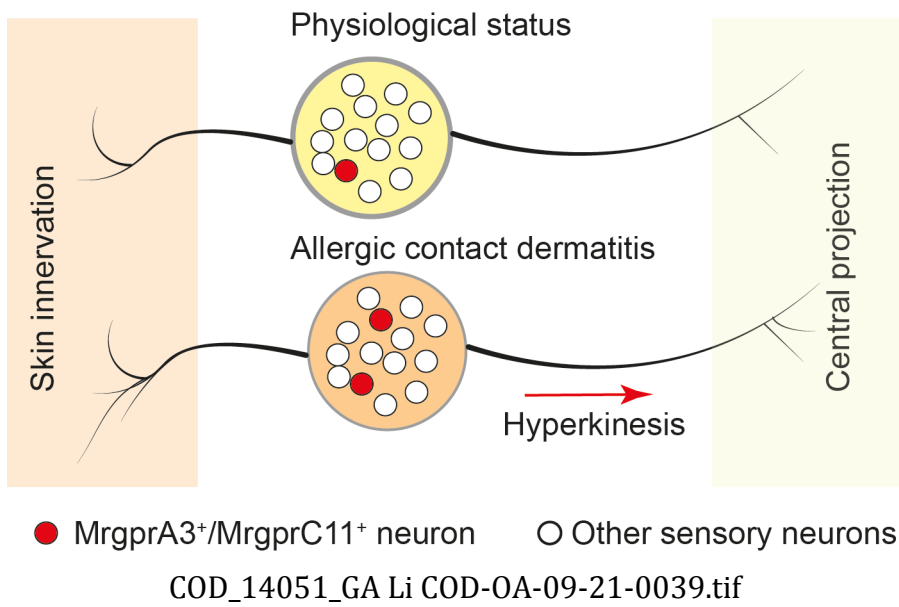


COD_14051_Figure4 bam AND cq calcium imaging-4.tif



COD_14051_Figure5 bam AND CQ injection-4.tif





- Oxazolone-induced allergic contact dermatitis (ACD) pruritus is partly depended on the expression of Mrgprs.
- ACD induces chronic itch and hyperkinesis through enhancing the expression and the activity of MrgprC11 and MrgprA3 in DRG neurons.
- *hMrgprX1* rescues diminished scratching behavior of *Mrgpr-clusterΔ^{-/-}* mice in ACD, and pharmacologically blocked hMrgprX1 by an antagonist (JHU739) significantly attenuated ACD-associated itch.